Disorder-Induced Long-Ranged Correlations in Scalar Active Matter

Sunghan Ro[1], Yariv Kafri,[1] Mehran Kardar[2] and Julien Tailleur[3]

[1]*Department of Physics, Technion-Israel Institute of Technology, Haifa 3200003, Israel*
[2]*Department of Physics, Massachusetts Institute of Technology, Cambridge, Massachusetts 02139, USA*
[3]*Université de Paris, laboratoire Matière et Systèmes Complexes (MSC), UMR 7057 CNRS, 75205 Paris, France*

We study the impact of quenched random potentials and torques on scalar active matter. Microscopic simulations reveal that motility-induced phase separation is replaced in two dimensions by an asymptotically homogeneous phase with anomalous long-ranged correlations and nonvanishing steady-state currents. Using a combination of phenomenological models and a field-theoretical treatment, we show the existence of a lower-critical dimension $d_c = 4$, below which phase separation is only observed for systems smaller than an Imry-Ma length scale. We identify a weak-disorder regime in which the structure factor scales as $S(q) \sim 1/q^2$, which accounts for our numerics. In $d = 2$, we predict that, at larger scales, the behavior should cross over to a strong-disorder regime. In $d > 2$, these two regimes exist separately, depending on the strength of the potential.

The influence of disorder on active systems has attracted a lot of interest recently [1–14]. In particular, long-range order has shown a surprising stability against the introduction of quenched disorder [15–21]. For systems belonging to the Vicsek universality class, where the order parameter has a continuous symmetry, the lower-critical dimension was shown to be $d_c = 2$: long-ranged polar order is observed in $d = 3$ and quasi-long-ranged order in $d = 2$ [16–18]. This makes such active systems *more robust* to disorder than equilibrium ones with a continuous symmetry, for which $d_c = 4$ [22–28].

While a lot of effort has been devoted to polar aligning active matter, comparatively less is known on the influence of disorder on the collective properties of scalar active matter, when the sole hydrodynamic mode is the density field. There, the combination of self-propulsion and kinetic hindrance leads to motility-induced phase separation (MIPS), even in the absence of attractive interactions, in dimensions $d \geq 2$ [29–46]. Despite important differences, MIPS shares many features of an equilibrium liquid-gas phase separation. The latter is stable to disorder above a lower-critical dimension $d_c = 2$, and it is natural to ask whether the same holds for MIPS.

In this Letter, we address this question by studying model systems of scalar active matter in the presence of quenched random potentials and torques using a combination of analytical and numerical approaches. The relevance of our results to experimental systems is discussed in the Conclusion. We show that MIPS is destroyed for $d \leq d_c$ with $d_c = 4$: The system only looks phase separated below an Imry-Ma length scale. Instead, disorder leads to asymptotically homogeneous systems with persistent steady-state currents. For $d > 2$, the system is either in a weak- or strong-disorder regime depending on the strength of the random potential. In the weak-disorder regime, the system is shown to exhibit self-similar correlations with a structure factor decaying as a power law, $S(q) \sim q^{-2}$, at small wave numbers q. This behavior is very different from that of an equilibrium scalar system, where correlations are short ranged with a structure factor behaving as a Lorentzian squared [28,47]. In $d = 2$, we instead predict a crossover between weak- and strong-disorder regimes at a length scale that we identify. Numerically we only observe the weak-disorder regime, in which we measure a pair-correlation function that decays logarithmically, in agreement with our analytical predictions. Interestingly, our results show that, contrary to what was reported for the transition to collective motion [16,17], scalar active systems are more fragile to disorder than passive ones. Our results are presented for random potentials but naturally extend to random torques, as shown in the Supplemental Material [48].

Numerical simulations.—We start by presenting results from numerical simulations of N run-and-tumble particles (RTPs) with excluded volume interactions on a two-dimensional lattice [42–44,51,52] of size $L \times L$ and periodic boundary conditions. Each particle has an orientation $\hat{e}_\theta = (\cos\theta, \sin\theta)$ with $\theta \in [0, 2\pi)$ and reorients to a new random direction with rate α. In the absence of disorder, activity is accounted for by hops from the position $\vec{i}$ of a particle to any neighboring site $\vec{j} = \vec{i} + \hat{u}$ with rate $W_{\vec{i},\vec{j}} = \max[v\hat{u} \cdot \hat{e}_\theta, 0]$, where v controls the propulsion speed. Interactions between the particles are accounted for by modifying the hopping rates according to $W_{\vec{i},\vec{j}}^{\text{int}} = W_{\vec{i},\vec{j}}(1 - n_{\vec{j}}/n_M)$ with $n_{\vec{j}}$ as the number of particles at $\vec{j}$
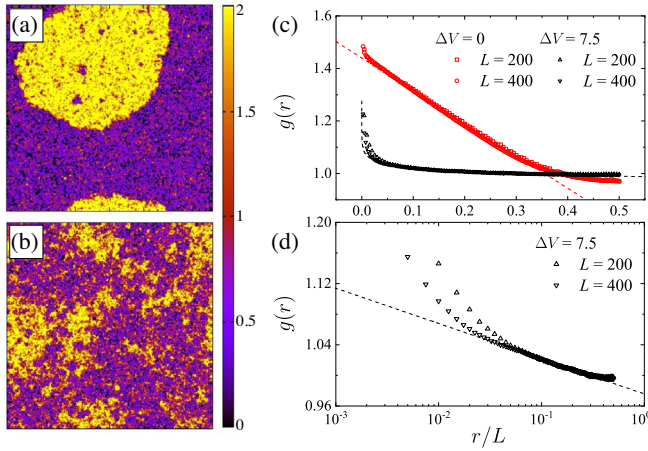
FIG. 1. Snapshots of simulations (a) without and (b) with disorder. Color encodes density, obtained by averaging occupancies over four neighboring sites. (c) The pair correlation functions are shown in linear scale with (black) and without (red) disorder. (d) Pair correlation with disorder using log-linear scale. The dashed lines correspond to linear (red) and logarithmic (black) decays. Parameters: (a),(b) $L = 300$; (b) $\Delta V = 7.5$; $v = 13$, $\alpha = 1$, $n_M = 2$, $\rho_0 \equiv N/L^2 = 1$.

and n_M as the maximal occupancy. For large enough v/α and densities, as shown in Fig. 1(a), the system displays MIPS [42]. The quenched disorder is modeled using $W_{\vec{i},\vec{j}} = \max\left[v\hat{u} \cdot \hat{e}_\theta - (V_{\vec{j}} - V_{\vec{i}}), 0\right]$ with $V_{\vec{i}}$ a random potential drawn from a *bounded* uniform distribution $V_{\vec{i}} \in [-\Delta V, \Delta V]$. Here, the lattice spacing and the mobility are set to one.

Surprisingly, Fig. 1(b) suggests that the phase separation is washed out by the random potential. The resulting disordered phase displays, however, a nontrivial structure, suggestive of interesting correlations. We quantify the latter using the pair-correlation function $g(r) = \overline{(1/L^2) \sum_j \langle n_{\vec{j}} n_{\vec{j}+\vec{r}} \rangle}$ where $r \equiv |\vec{r}|$, the brackets represent a steady-state average, and the overline denotes an average over disorder realizations. In the absence of disorder, phase separation translates into a linear decay of $g(r)$, as shown in Fig. 1(c). On the contrary, in the presence of disorder, the correlations are found to decay logarithmically, $g(r) \sim \log(L/r)$, as shown in Fig. 1(d). This corresponds to a structure factor $S(q) \sim q^{-2}$ for small q.

To explain the disappearance of phase separation and the emergence of nontrivial correlations, we first introduce a phenomenological model that captures the latter in a dilute system. This then suggests a field-theoretic perspective that predicts the existence of weak- and strong-disorder regimes. It first allows us to characterize the disorder-induced persistent currents that flow in the system and then to come back to the arrest of MIPS. Using the field theory, we identify the lower-critical dimension as $d_c = 4$ and estimate the Imry-Ma length scale above which phase separation is arrested in $d < 4$.

Phenomenological model for a dilute system.—Random potential and torques impact many aspects of the single-particle dynamics. As we show, all the emerging phenomenology reported here can be traced back to a single aspect: the emergence of ratchet currents. When a localized asymmetric potential centered around $\mathbf{r}_0$ is placed in an active fluid of noninteracting RTPs, the stationary density field $\langle \rho(\mathbf{r}) \rangle$ in the far field of the potential is [53]

$$\langle \rho(\mathbf{r}) \rangle = \rho_0 + \frac{\beta_{\text{eff}}}{S_d} \frac{(\mathbf{r} - \mathbf{r}_0) \cdot \mathbf{p}}{|\mathbf{r} - \mathbf{r}_0|^d} + \mathcal{O}(|\mathbf{r} - \mathbf{r}_0|^{-d}). \quad (1)$$

Here, $S_d = 2\pi^{d/2}/\Gamma(d/2)$, ρ_0 is the density of the active fluid, $\beta_{\text{eff}} \equiv 2\alpha/v^2$, and the mobility of the particles is set to one. The vector $\mathbf{p}$ is given by the average force exerted by the potential on the active fluid and is thus proportional to the overall density. In the presence of torques, Eq. (1) still holds but with a renormalized $\mathbf{p}$ [48]. Given the analogy between Eq. (1) and electrostatics, we follow Ref. [53] and refer to the force $\mathbf{p}$ as a dipole.

With Eq. (1) in mind, we consider a phenomenological model in which the bounded random potential is modeled as a superposition of random independent dipoles. Each dipole exerts a force on the active particles in a direction dictated by the local potential, as sketched in Figs. 2(a) and 2(b). To test this random dipole picture numerically, we measure in Fig. 2(c) the force $f(A)$ exerted along an arbitrary direction by the random potential on the particles inside an area A. Consistent with our phenomenological model, $f(A)$ scales as $\sqrt{A}$. This should be contrasted with equilibrium systems, where $f(A)$ is expected to scale as $A^{1/4}$. Indeed, a random bounded potential $V(\mathbf{r})$ leads, in equilibrium, to a force density $\propto \beta^{-1}\rho_0\nabla\exp(-\beta V)$. Integrating over an area A solely leads to a boundary
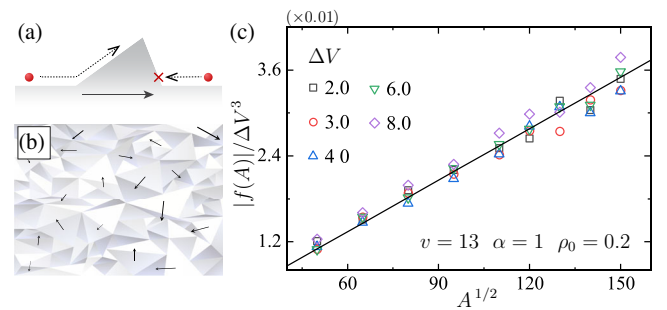

FIG. 2. (a) In $d = 1$, asymmetric potentials leads to a nonzero average force on the particles, indicated by a bold arrow. This is accompanied by a nonvanishing ratchet current. (b) In $d = 2$, a random potential leads to a steady-state field of random forces exerted on the particles. (c) Measurement of the force $f(A)$ exerted on the active particles inside a region of area A in the presence of a random potential. The amplitude of the force is quantified by $|f(A)| \equiv [\overline{f^2(A)}]^{1/2}$, where $f(A)$ is obtained by time averaging $\sum_{\vec{i}\in A} n_{\vec{i}}(V_{\vec{i}+\vec{e}} - V_{\vec{i}-\vec{e}})/2$ with $\vec{e}$ as an arbitrary unit vector.

contribution proportional to $\int_{\partial A} \exp(-\beta V)\vec{n}d\ell$. Only the fluctuations of $V(\mathbf{r})$ contribute, leading to the $A^{1/4}$ scaling. Figure 2(c) thus highlights the nonequilibrium nature of the system: the ratchet effect induced by the random potential leads to an emerging force field with short-range correlations. Finally, the scaling of $F(A)$ as ΔV^3 in this dilute regime is consistent with a perturbative result, which predicts $|\mathbf{p}| \sim \Delta V^3$ as $\Delta V \to 0$ [53], despite the relatively large values of ΔV used here.

We now use the phenomenological model to predict the structure factor based on the random dipole picture. The dipole density field $\mathbf{P}(\mathbf{r})$ is randomly drawn from a distribution such that the spatial components of $\mathbf{P}$ satisfy $\overline{P_i(\mathbf{r})} = 0$ and $\overline{P_i(\mathbf{r})P_j(\mathbf{r}')} = \chi^2\delta_{ij}\delta^d(\mathbf{r}-\mathbf{r}')$, notably lacking spatial correlations in $\mathbf{P}(\mathbf{r})$. Denoting $\langle\phi(\mathbf{r})\rangle \equiv \langle\rho(\mathbf{r})\rangle - \rho_0$, a direct computation, detailed in [48], leads from Eq. (1) to the disorder-averaged structure factor

$$S(\mathbf{q}) \equiv \overline{\langle\phi(\mathbf{q})\phi(-\mathbf{q})\rangle} = \frac{\beta_{\text{eff}}^2\chi^2}{q^2}, \qquad (2)$$

with $q \equiv |\mathbf{q}|$. Note that, in the dilute (noninteracting) regime, the computation simplifies thanks to $S(\mathbf{q}) = \overline{\langle\phi(\mathbf{q})\rangle\langle\phi(-\mathbf{q})\rangle}$. Including interactions between the particles is possible at the level of Eq. (1) [54], which would only change the prefactor of q^{-2} in Eq. (2). We stress that these predictions, illustrated for scalar active matter, should hold for many active systems, including polar and nematic ones, in the disordered phase. In [48] we indeed report long-range correlations in a dilute system with aligning interactions.

Remarkably, the functional form of $S(\mathbf{q})$ predicted by the phenomenological model agrees well with our numerics even when the particle density is not small, see Fig. 1(d). Building on the successful predictions of the phenomenological model, we now propose a field-theoretical description of scalar active matter subject to quenched random potentials.

Field-theoretic treatment.—Our results suggest that the overall density is homogeneous at large scales, with small fluctuations, so that the system can be described by a linear field theory. This assumption will be checked in the section on the strong-disorder regime using a self-consistency criterion. To model the force field emerging from the ratchet effect due to the bounded random potential $V(\mathbf{r})$, we introduce a quenched *random force* density $\mathbf{f}(\mathbf{r})$ acting on the active fluid. We consider the dynamics

$$\frac{\partial}{\partial t}\phi(\mathbf{r},t) = -\nabla\cdot\mathbf{j}(\mathbf{r},t), \qquad (3)$$

$$\mathbf{j}(\mathbf{r},t) = -\nabla\mu[\phi] + \mathbf{f}(\mathbf{r}) + \sqrt{2D}\boldsymbol{\eta}(\mathbf{r},t), \qquad (4)$$

where $\phi(\mathbf{r},t)$ denotes density fluctuations, $\mathbf{j}(\mathbf{r},t)$ is the linearized current, and $\boldsymbol{\eta}(\mathbf{r},t)$ is a unit Gaussian white noise field. The mobility is set to one and the random force density satisfies $\overline{f_i(\mathbf{r})} = 0$ and $\overline{f_i(\mathbf{r})f_j(\mathbf{r}')} = \sigma^2\delta_{ij}\delta^d(\mathbf{r}-\mathbf{r}')$. To linear order in ϕ we set

$$\mu[\phi(\mathbf{r},t)] = u\phi(\mathbf{r},t) - K\nabla^2\phi(\mathbf{r},t), \qquad (5)$$

with $u, K > 0$ to ensure stability. Note that, in the small-fluctuation regime, $\boldsymbol{\eta}$ and $\mathbf{f}$ are independent of ϕ, while σ, D, u, and K generically depend on the mean density ρ_0. Much work has been done, in other contexts, on a single-particle subject to a random force [55,56]. Our results complement these classical works at the level of collective modes. The structure factor is then given by [48]

$$S(\mathbf{q}) = \frac{\sigma^2}{q^2(u+Kq^2)^2} + \frac{D}{(u+Kq^2)}. \qquad (6)$$

Note that the small q behavior of the structure factor reproduces the scaling $S(q) \propto q^{-2}$ predicted by the phenomenological model and observed in the numerics of Fig. 1. In fact, comparing Eqs. (2) and (6) shows that σ/u is proportional, in the dilute regime, to the inverse effective temperature: $\sigma/u \propto \chi\beta_{\text{eff}}$ [57]. Interestingly, noise and interactions are subleading as $q \to 0$.

To further understand this result, we use a Helmholtz-Hodge decomposition of the random force field: $\mathbf{f}(\mathbf{r}) = -\nabla U(\mathbf{r}) + \boldsymbol{\xi}(\mathbf{r})$. Here $U(\mathbf{r})$ is an effective potential reconstructed from the random force. Its statistical properties, as we show below, are very different from those of the potential $V(\mathbf{r})$ which is short-range correlated. The reconstructed vector field $\boldsymbol{\xi}(\mathbf{r})$ satisfies $\nabla\cdot\boldsymbol{\xi}(\mathbf{r}) = 0$, so that it impacts the current $\mathbf{j}$ but does not influence the dynamics of the density field. To enforce the delta correlations of $\mathbf{f}(\mathbf{r})$ together with its statistics, we set $\overline{U(\mathbf{q})U(\mathbf{q}')} = \sigma^2 q^{-2}\delta_{\mathbf{q},-\mathbf{q}'}^d$, $\overline{\xi_i(\mathbf{q})\xi_j(\mathbf{q}')} = \sigma^2(\delta_{ij} - q_iq_j'/q^2)\delta_{\mathbf{q},-\mathbf{q}'}^d$, and $\overline{U(\mathbf{q})\boldsymbol{\xi}(\mathbf{q}')} = 0$ so that U and $\boldsymbol{\xi}$ are intimately related. Inserting the decomposition into Eqs. (3) and (4) shows that the density fluctuations of active particles in the disordered setting behave as those of passive particles in an effective potential $U(\mathbf{r})$. The statistics of $U(\mathbf{r})$ are those of a Gaussian surface [59]—a self-affine fractal with deep wells. This effective potential captures the component of the nonequilibrium current $\mathbf{j}$, which accounts for both the clustering and the long-range correlations observed in our numerics. [See Fig. 1(b) and Supplemental Videos [48], which show how MIPS is destabilized by the introduction of the random potential].

Persistent currents.—The random force density $\mathbf{f}(\mathbf{r})$ is a nonconservative vector field due to the divergence-free part $\boldsymbol{\xi}(\mathbf{r})$. While this term does not influence the density field, it induces currents in the system. To quantify them, we consider a closed contour $\mathcal{C}$. Taking the curl of the total current and averaging over noise, one finds $\langle\nabla\times\mathbf{j}\rangle = \nabla\times\boldsymbol{\xi}$. Integrating this relation over a domain
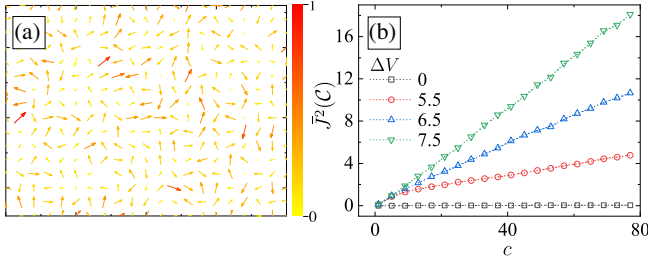
FIG. 3. The current induced by disorder and its statistical properties. (a) Current vector map for a realization of disorder. The color code is the steady-state current normalized by the maximum value measured. (b) The variance of the sum of current $J(\mathcal{C})$ along a contour $\mathcal{C}$ as a function of the its perimeter c. Parameters: $v = 13$, $\alpha = 1$, $\Delta V = 6.5$ in (a).

enclosed by $\mathcal{C}$, we obtain, using Stokes' theorem, that the circulation of $\langle \mathbf{j} \rangle$ is entirely controlled by $\boldsymbol{\xi}$: $J(\mathcal{C}) \equiv \oint_{\mathcal{C}} d\mathbf{l} \cdot \mathbf{j}(\mathbf{r}) = \oint_{\mathcal{C}} d\mathbf{l} \cdot \boldsymbol{\xi}(\mathbf{r})$. $J(\mathcal{C})$ is thus a sum of uncorrelated random numbers and we predict its variance to scale as the perimeter of the contour $\mathcal{C}$, with a slope proportional to the disorder strength σ. This is confirmed by our numerics in Fig. 3(b). Furthermore, the steady-state current induced by a realization of the random potential is shown in Fig. 3(a). It should be contrasted with the equilibrium case in which currents vanish in the steady state.

Strong-disorder regime and self-consistency of the linear theory.—The linear theory used in the previous section is valid as long as density fluctuations are small compared to the mean density. To detect a possible departure from this scenario, we measure the density fluctuations across a length ℓ through $\overline{\langle \delta\rho^2(\ell) \rangle} = 2[g(a) - g(\ell)]$, where a is a short-distance cutoff. The fluctuations have to remain small compared to the natural scales of the density field: $\overline{\langle \delta\rho^2(\ell) \rangle} \ll \rho_b^2$ with $\rho_b \equiv \min(\rho_0, \rho_M - \rho_0)$. Here ρ_0 and ρ_M are the average and maximal particle densities. Using Eq. (6), we find for large ℓ

$$\frac{\overline{\langle \delta\rho^2(\ell) \rangle}}{\rho_b^2} = \begin{cases} \frac{\sigma^2 \ln(\ell/a)}{\pi u^2 \rho_b^2} & \text{for } d = 2 \\ \frac{\sigma^2 a^{2-d}}{(d-2)S_d u^2 \rho_b^2} & \text{for } d > 2. \end{cases} \quad (7)$$

For $d > 2$, the linear theory thus holds if $\sigma \ll u\rho_b\sqrt{(d-2)S_d a^{d-2}}$, namely, whenever the disorder is weak enough. For strong enough disorder, the breakdown of the linear approximation indicates the possibility of a different behavior for $S(q)$. For $d = 2$, the criterion is valid only for length scales satisfying $\ell \ll \ell^*$ with $\ell^* \equiv a \exp(\pi u^2 \rho_b^2 / \sigma^2)$. Note that this length scale is exponential in the square of the ratio between the effective temperature and the disorder strength, since $\sigma/u \propto \beta_{\text{eff}}\chi$. This can be estimated using Fig. 2, leading to very large length scales, well beyond the reach of our numerics.

We suggest in the Supplemental Material [48] an alternative numerical approach to study the strong-disorder regime in $d = 2$ using passive particles in a Gaussian surface. The resulting correlation function shows clear deviations from the logarithmic behavior on large length scales.

Lower-critical dimension.—Our linear theory offers an avenue to test the stability of phase separation against weak disorder. To do so, we note that the Helmholtz-Hodge decomposition implies that the dynamics of $\phi(\mathbf{r})$ are similar to an equilibrium dynamics in a correlated random potential $U(\mathbf{r})$. This allows employing an Imry-Ma argument [22,23] in order to obtain the lower-critical dimension d_c below which phase separation is suppressed at large scales. To do so, we consider a domain of linear size ℓ. The surface energy of the domain is given by $\gamma \ell^{d-1}$, with γ as the surface tension [60]. On the other hand, the contribution of the disorder to the energy of the domain is, to leading order, $E(\ell) = \int_{\ell^d} d^d\mathbf{r}' \rho_0 U(\mathbf{r}')$. The typical energy of a domain of size ℓ is thus given by $\sqrt{\overline{E(\ell)^2}} = \sigma\rho_0 \ell^{(d+2)/2}$. Comparing the two energy scales shows the lower-critical dimension to be $d_c = 4$. In lower dimensions, the contribution of the surface energy is negligible on large enough length scales and a system of size L does not phase separate if $L \gg \ell_{\text{IM}} \simeq [\gamma/(\sigma\rho_0)]^{2/(4-d)}$, which we call the Imry-Ma length scale. Numerically, we indeed confirm that the coarsening to a single macroscopic domain is only observed for small system sizes. Correspondingly, a transition from linearly decaying to logarithmically decaying pair-correlation functions with increasing L is reported in the Supplemental Material [48].

Note that the Imry-Ma argument rules out the existence of a macroscopic ordered, dense phase. Alternatively, the absence of MIPS could stem from the suppression of the feedback loop between a slowdown of particles at high density and their tendency to accumulate where they move slower. Reformulated as a mean-field theory, this feedback loop translates into an instability criteria for a homogeneous system of density ρ whenever $\rho v'(\rho) < -v(\rho)$ [29,38], where $v(\rho)$ is an effective propulsion speed in a system of density ρ. We report in Fig. 4 the measurement of $v(\rho)$ for our system, defined as the mean hopping rate of particles along their orientation, with and without the
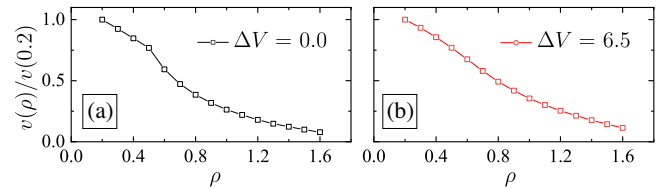

FIG. 4. Measurement of the effective self-propulsion speed $v(\rho)$ in our simulations (a) without and (b) with disorder for $v = 13$ and $\alpha = 1$. Both systems exhibit a similar decay that, in the absence of disorder, would lead to MIPS. Note that the kink observed for $v(\rho)$ in (a) stems from the occurrence of phase separation.

random potential. Both systems show a similar decay which, at mean-field level, would predict the occurrence of MIPS. It is thus the nontrivial correlations induced by disorder that make MIPS disappear at large scales, despite an underlying instability at mean-field level. The disorder-induced disappearance of MIPS thus has a very different origin than its arrest by diffusiophoretic [62,63] or hydro-dynamic [64] interactions that directly prevent a kinetic hindrance at the microscopic scale.

Conclusion.—In this Letter, we have shown how random quenched potentials and torques lead to a nontrivial phase in scalar active matter with anomalous correlations that prevent phase separation. Interestingly, while the transition to collective motion is more robust to disorder than the corresponding ferromagnetic transition in equilibrium [16,17], the converse holds for scalar phase separation: the lower-critical dimension is larger in the active case ($d_c = 4$) than in the passive one ($d_c = 2$). We also note a strong difference between the one-dimensional active case, in which disorder promotes clustering [10], and the two-dimensional one, in which MIPS is destroyed by disorder at large scale. We expect our results, presented here for RTPs, to hold for generic scalar active systems, including active Brownian and active Ornstein Uhlenbeck particles. Experimentally, we expect our results to be relevant for a large class of systems. Long-ranged correlations, forces on obstacles, and current circulations could be tested using self-propelled colloids [65,66] and shaken grains [67] on irregular surfaces—at least in their dilute, disordered phase—as well as swimming bacteria in disordered media [12,13]. The suppression of phase separation and MIPS-related physics could be studied in experiments using self-propelled colloids [31,68] or bacteria [69,70]. It would also be of interest to see whether the bubbly phase, uncovered recently in [41,61], exhibits different behavior under disorder. Finally, we note that random potentials lead to ratchets in many nonequilibrium systems, whether classical or quantum, far beyond the realm of active matter. Since these currents are the building blocks of our field-theoretical treatment, we expect our results to play a role in many nonequilibrium systems experiencing random potentials.

[1] O. Chepizhko and F. Peruani, Phys. Rev. Lett. **111,** 160604 (2013).

[2] C. Reichhardt and C. J. Olson Reichhardt, Phys. Rev. E **90,** 012701 (2014).

[3] C. Bechinger, R. Di Leonardo, H. Lowen, C. Reichhardt, G. Volpe, and G. Volpe, Rev. Mod. Phys. **88,** 045006 (2016).

[4] E. Pine, S. K. P. Velu, A. Callegari, P. Elahi, S. Gigan, G. Volpe, and G. Volpe, Nat. Commun. **7,** 10907 (2016).

[5] A. Morin, D. Lopes Cardozo, V. Chikkadi, and D. Bartolo, Phys. Rev. E **96,** 042611 (2017).

[6] C. Sandor, A. Libal, C. Reichhardt, and C. J. Olson Reichhardt, Phys. Rev. E **95,** 032606 (2017).

[7] F. Peruani and I. S. Aranson, Phys. Rev. Lett. **120,** 238101 (2018).

[8] C. Reichhardt and C. J. O. Reichhardt, Phys. Rev. E **97,** 052613 (2018).

[9] R. L. Stoop and P. Tierno, Commun. Phys. **1,** 68 (2018).

[10] Y. Ben Dor, E. Woillez, Y. Kafri, M. Kardar, and A. P. Solon, Phys. Rev. E **100,** 052610 (2019).

[11] P. L. Doussal, S. N. Majumdar, and G. Schehr, Europhys. Lett. **130,** 40002 (2020).

[12] T. Bhattacharjee and S. S. Datta, Soft Matter **15,** 9920 (2019).

[13] T. Bhattacharjee and S. S. Datta, Nat. Commun. **10,** 2075 (2019).

[14] E. Woillez, Y. Kafri, and N. S. Gov, Phys. Rev. Lett. **124,** 118002 (2020).

[15] R. Das, M. Kumar, and S. Mishra, Phys. Rev. E **98,** 060602 (R) (2018).

[16] J. Toner, N. Guttenberg, and Y. Tu, Phys. Rev. E **98,** 062604 (2018).

[17] J. Toner, N. Guttenberg, and Y. Tu, Phys. Rev. Lett. **121,** 248002 (2018).

[18] A. Maitra, Phys. Rev. E **101,** 012605 (2020).

[19] O. Chepizhko, E. G. Altmann, and F. Peruani, Phys. Rev. Lett. **110,** 238101 (2013).

[20] A. Morin, N. Desreumaux, J.-B. Caussin, and D. Bartolo, Nat. Phys. **13,** 63 (2017).

[21] A. Chardac, S. Shankar, M. C. Marchetti, and D. Bartolo, arXiv:2002.12893.

[22] Y. Imry and S.-k. Ma, Phys. Rev. Lett. **35,** 1399 (1975).

[23] A. Aharony, Y. Imry, and S.-k. Ma, Phys. Rev. Lett. **37,** 1364 (1976).

[24] D. S. Fisher, J. Frhlich, and T. Spencer, J. Stat. Phys. **34,** 863 (1984).

[25] D. P. Belanger, A. R. King, V. Jaccarino, and J. L. Cardy, Phys. Rev. B **28,** 2522 (1983).

[26] J. Z. Imbrie, Phys. Rev. Lett. **53,** 1747 (1984).

[27] J. Bricmont and A. Kupiainen, Phys. Rev. Lett. **59,** 1829 (1987).

[28] U. Glaus, Phys. Rev. B **34,** 3203 (1986).

[29] J. Tailleur and M. E. Cates, Phys. Rev. Lett. **100,** 218103 (2008).

[30] Y. Fily and M. C. Marchetti, Phys. Rev. Lett. **108,** 235702 (2012).

[31] I. Buttinoni, J. Bialke, F. Kummel, H. Lowen, C. Bechinger, and T. Speck, Phys. Rev. Lett. **110,** 238301 (2013).

[32] M. E. Cates and J. Tailleur, Europhys. Lett. **101,** 20010 (2013).

[33] J. Stenhammar, A. Tiribocchi, R. J. Allen, D. Marenduzzo, and M. E. Cates, Phys. Rev. Lett. **111,** 145702 (2013).

[34] G. S. Redner, M. F. Hagan, and A. Baskaran, Phys. Rev. Lett. **110,** 055701 (2013).

[35] A. P. Solon, M. E. Cates, and J. Tailleur, Eur. Phys. J. Special Topics **224**, 1231 (2015).

[36] G. S. Redner, C. G. Wagner, A. Baskaran, and M. F. Hagan, Phys. Rev. Lett. **117**, 148002 (2016).

[37] S. Paliwal, J. Rodenburg, R. van Roij, and M. Dijkstra, New J. Phys. **20**, 015003 (2018).

[38] M. E. Cates and J. Tailleur, Annu. Rev. Condens. Matter Phys. **6**, 219 (2015).

[39] A. P. Solon, J. Stenhammar, M. E. Cates, Y. Kafri, and J. Tailleur, Phys. Rev. E **97**, 020602(R) (2018).

[40] A. P. Solon, J. Stenhammar, M. E. Cates, Y. Kafri, and J. Tailleur, New J. Phys. **20**, 075001 (2018).

[41] E. Tjhung, C. Nardini, and M. E. Cates, Phys. Rev. X **8**, 031080 (2018).

[42] A. G. Thompson, J. Tailleur, M. E. Cates, and R. A. Blythe, J. Stat. Mech. (2011) P02029.

[43] M. Kourbane-Houssene, C. Erignoux, T. Bodineau, and J. Tailleur, Phys. Rev. Lett. **120**, 268003 (2018).

[44] S. Whitelam, K. Klymko, and D. Mandal, J. Chem. Phys. **148**, 154902 (2018).

[45] J. Palacci, S. Sacanna, A. P. Steinberg, D. J. Pine, and P. M. Chaikin, Science **339**, 936 (2013).

[46] D. Geyer, D. Martin, J. Tailleur, and D. Bartolo, Phys. Rev. X **9**, 031043 (2019).

[47] M. Kardar, *Statistical Physics of Fields* (Cambridge University Press, Cambridge, England, 2007).

[48] See Supplemental Material at http://link.aps.org/supplemental/10.1103/PhysRevLett.126.048003, which also includes descriptions of the videos and references to [49,50].

[49] A. P. Solon, Y. Fily, A. Baskaran, M. E. Cates, Y. Kafri, M. Kardar, and J. Tailleur, Nat. Phys. **11**, 673 (2015).

[50] Y. Fily, Y. Kafri, A. P. Solon, J. Tailleur, and A. Turner, J. Phys. A **51**, 044003 (2018).

[51] R. Soto and R. Golestanian, Phys. Rev. E **89**, 012706 (2014).

[52] N. Sepúlveda and R. Soto, Phys. Rev. E **94**, 022603 (2016).

[53] Y. Baek, A. P. Solon, X. Xu, N. Nikola, and Y. Kafri, Phys. Rev. Lett. **120**, 058002 (2018).

[54] O. Granek, Y. Baek, Y. Kafri, and A. P. Solon, J. Stat. Mech. (2020) 063211.

[55] D. S. Fisher, Phys. Rev. A **30**, 960 (1984).

[56] J.-P. Bouchaud, A. Comtet, A. Georges, and P. Le Doussal, Ann. Phys. (N.Y.) **201**, 285 (1990).

[57] With interactions, one finds $\chi/P'(\rho_0) = \sigma/u$, with P as the pressure of the active fluid [54,58].

[58] A. P. Solon, J. Stenhammar, R. Wittkowski, M. Kardar, Y. Kafri, M. E. Cates, and J. Tailleur, Phys. Rev. Lett. **114**, 198301 (2015).

[59] $U(\mathbf{r})$ can be constructed from $\mathbf{f}(\mathbf{r})$ by solving $\nabla^2 U(\mathbf{r}) = \nabla \cdot \mathbf{f}(\mathbf{r})$.

[60] Unlike equilibrium systems, γ, when defined through momentum fluxes, can be negative for scalar active matter with pairwise forces, leading to a bubbly liquid phase [41,61]. We expect our result to hold provided that the cost of the domain wall in the steady-state distribution increases as ℓ^{d-1} which is needed for overall phase separation between dilute gas and bubbly liquid phases.

[61] X.-q. Shi, G. Fausti, H. Chate, C. Nardini, and A. Solon, Phys. Rev. Lett. **125**, 168001 (2020).

[62] O. Pohl and H. Stark, Phys. Rev. Lett. **112**, 238303 (2014).

[63] A. Zöttl and H. Stark, Phys. Rev. Lett. **112**, 118101 (2014).

[64] R. Matas-Navarro, R. Golestanian, T. B. Liverpool, and S. M. Fielding, Phys. Rev. E **90**, 032304 (2014).

[65] J. R. Howse, R. A. L. Jones, A. J. Ryan, T. Gough, R. Vafabakhsh, and R. Golestanian, Phys. Rev. Lett. **99**, 048102 (2007).

[66] A. Bricard, J.-B. Caussin, N. Desreumaux, O. Dauchot, and D. Bartolo, Nature (London) **503**, 95 (2013).

[67] J. Deseigne, O. Dauchot, and H. Chaté, Phys. Rev. Lett. **105**, 098001 (2010).

[68] M. N. van der Linden, L. C. Alexander, D. G. A. L. Aarts, and O. Dauchot, Phys. Rev. Lett. **123**, 098001 (2019).

[69] G. Liu, A. Patch, F. Bahar, D. Yllanes, R. D. Welch, M. C. Marchetti, S. Thutupalli, and J. W. Shaevitz, Phys. Rev. Lett. **122**, 248102 (2019).

[70] A. Curatolo, N. Zhou, Y. Zhao, C. Liu, A. Daerr, J. Tailleur, and J. Huang, Nat. Phys. **16**, 1152 (2020).